

CHAPTER 3 «PROPAGATION OF THE TERAHERTZ LASER RADIATION WITH SPATIALLY INHOMOGENEOUS POLARIZATION IN DIFFERENT ZONES OF DIFFRACTION»DOI: <https://doi.org/10.30525/978-9934-26-461-0-3>

The development of micro- and nanotechnologies requires new methods of formation and research of light fields with subwavelength dimensions of energy localization regions. Such problems are characterized by nonparaxial propagation of light and the impossibility of applying the scalar approximation. The distribution of electric field energy by components and, as a consequence, the polarization characteristics of radiation come to the fore.

Light beams are narrowly directed light radiation that spreads in a small body angle. If the beam divergence angle is small, $\theta \sim 10^{-3} - 10^{-2}$, such a beam is called paraxial. In paraxial beams, the longitudinal component of the field is much smaller than the transverse components. Therefore, paraxial beams are usually described by one transverse component of the field. Such beams are called scalar. Most often, paraxial light beams are described as scalar, which is quite sufficient in most cases. Such a deliberately simplified approach is often used when describing the properties of light beams [104; 105]. However, for beams in which the divergence angle is large, the scalar approximation is not sufficient. Moreover, even for paraxial light beams, in which the polarization is nonuniform across the cross section, it is necessary to use a stricter vector formalism. Finally, the scalar approximation in all cases does not allow naturally describing the vector characteristics of the beam. It is more general to describe laser light beams as three-dimensional vector fields. However, vector beams have been studied much less (see, for example, [106]).

In [107], it was shown that when analyzing the diffraction of radiation beams, a zero value of the intensity on the optical axis is possible due to the presence of a longitudinal component of the field. Therefore, when studying the spatial-energy characteristics of laser beams, take into account the vector nature of the propagating radiation.

3.1. MODELING OF RADIATION PROPAGATION WITH INHOMOGENEOUS POLARIZATION IN DIFFERENT DIFFRACTION ZONES

In connection with the decrease in the size of laser systems, much attention has recently been paid to the description of nonparaxial propagation of light fields and the development of algorithms for modeling such propagation.

In [108], the propagation of a Gaussian beam in a homogeneous, isotropic, linear, and nonmagnetic dielectric medium was studied for the first time using the angular spectrum method. The electric field excited with a Gaussian beam in a dielectric medium is described by the expressions for the paraxial part and non-Gaussian correction terms of a higher order.

Characteristics for the propagation of azimuthally (or radially) polarized Lager-Gaussian beams for any optical systems described by the complex ABCD matrix were obtained [109]. These systems can have an arbitrary number of lenses, sections of free space and dielectrics, media with a radial amplification profile, spherical mirrors, reflectors. An analysis of the vector wave equation was carried out in [110]. A class of self-model solutions for the corresponding resonator modes with inhomogeneous polarization is derived. In [111] the solution of the Maxwell equations was proposed using the method of the plane wave spectrum of the electromagnetic field. In this representation, the solution of the electric field is written as the sum of two terms orthogonal to each other in the far zone. The concept of the near field to a given beam is introduced and applied to the known linearly polarized Gaussian beam.

In [112], the distribution of the field in the far zone, which is formed by the output ring modes with different polarization states, was studied using the Fresnel vector diffraction integral. It is shown that the azimuthal polarization is mainly transformed into radial during the propagation of ring beams with an azimuthal index above zero. This effect can contribute to increasing the productivity of a laser metal cutting system based on beams of this kind. In [113], the features of propagation in free space of light spirally polarized beams were studied in both paraxial and nonparaxial cases. Simple and important analytical results are obtained when the transverse intensity profile is chosen to correspond to a first-order axisymmetric Lager-Gaussian beam.

The polarization properties of vector coherent nonparaxial Gaussian beams are studied [114]. It is shown that when the radiation source of a nonparaxial Gaussian beam is fully polarized, the degree of polarization during field propagation maintains a constant value equal to unity. However, when the source is completely unpolarized, the degree of polarization during the propagation of the field does not keep a constant value, which is equal to zero. In [115], on the basis of the Rayleigh-Sommerfeld vector formula and using the relation between the Hermite and Lager polynomials, analytical expressions for the propagation of Hermite-Gaussian and Lager-Gaussian beams in the case of paraxial approximation are obtained with the corresponding expressions for propagation in the far zone, which are further derived for Gaussian beams as special cases of results. In [116], based on Rayleigh's vector diffraction integrals and the stationary phase method, an analytical expression was obtained that describes the propagation of the vector field of radially polarized Gaussian beams diffracted on an axicon.

The formula for the vector plane wave spectrum of an arbitrarily polarized electromagnetic wave in a homogeneous medium is derived using the method of mode decomposition of independent transverse fields [117]. This expression includes TM and TE modes for the spectrum of plane waves, where the amplitudes are separated and the polarization direction of each plane wave is given separately. In [118], based on the analysis of the vector structure of nonparaxial electromagnetic beams based on the stationary phase method, analytical expressions for the TE and TM modes of a linearly polarized Gaussian beam are presented in the nonparaxial approximation in the far zone. In [119], based on the Rayleigh-Sommerfeld vector formula, the nonparaxial propagation of radially polarized beams in free space was investigated analytically and with the help of numerical methods. An exact expression for describing the propagation of radially polarized light beams, which is valid for fields with an arbitrary transverse beam size, was obtained in a closed form for any point on the axis.

Based on the study of the vector structure of a electromagnetic beam and using the nonparaxial vector theory of moments, relations were presented for the beam radius, divergence angles and beam propagation factors in the nonparaxial case for a linearly polarized Gaussian beam and its TE and TM components [120]. In [121], a comparison of the results of calculations using the vector angular spectrum method and the Rayleigh-

Sommerfeld diffraction formula was made. On the basis of the angular spectrum method and the Weyl representation of a spherical wave, vector Rayleigh-Sommerfeld diffraction formulas of the first and second kind were obtained. In [122], analyzing the vector structure of an electromagnetic beam and using the stationary phase method, analytical expressions of the TE and TM components for a radially polarized Gaussian beam in the far zone were presented and a rigorous solution of Maxwell's equations was obtained for a confocal resonator. The components of the vector structure of the radially polarized Gaussian beam are compared with the components of the Gaussian TEM_{00} mode. Radially polarized "sophisticated" beams are considered in [123]. When describing such beams, the Lager polynomial has a complex argument, which is considered and analyzed. The features of the propagation of radially polarized beams in free space in the paraxial and nonparaxial cases are described from the point of view of the Rayleigh-Sommerfeld vector formula.

Using the vector angular spectrum method for an electromagnetic beam, the analytical vector structure of radially polarized beams is described [124]. The obtained results show that radially polarized beams consist only of TM waves. The concept of vector Lager-Bessel-Gaussian beams is proposed in [125]. On the basis of Rayleigh-Sommerfeld vector formulas, analytical formulas for the nonparaxial propagation of such vector beams were obtained [126] gives a description of a nonparaxial Gaussian beam based directly on Maxwell's equations. The vector angular spectrum method was used to solve these equations. Given the decomposition of the vector angular spectrum in the frequency domain into two terms, it is proposed to represent the nonparaxial Gaussian beam as the sum of two terms.

In [127], for a detailed description of the polarization features of nonparaxial radially polarized fields, a simple analytical propagation law using the method of the angular spectrum of plane waves is presented. Based on the parameter describing the width of the angular spectrum, a comparison was made between nonparaxial and paraxial results. In [128], using the angular spectrum method, general expressions were proposed to describe the propagation in free space of electromagnetic fields with a radial or azimuthal polarization structure in the transverse plane. The transverse distributions of the radial, azimuthal, and longitudinal components of these

fields were also analyzed. In particular, the features of the field on the axis during propagation in free space were studied.

Nonparaxial diffraction of Gaussian optical vortices with initial radial polarization was studied [129]. Explicit analytical expressions for the radial, azimuthal, and longitudinal components of the electric field intensity vector were obtained. Modeling showed that nonparaxial formulas describe the field much more accurately when moving away from the optical axis than paraxial ones. In [130], a general expression for the electric field of a cylindrically polarized vector beam propagating in free space was obtained on the basis of the exact vector solution of Maxwell's equations in the transverse Fourier plane. His analysis shows that the case of cylindrical polarization can be considered as a combination of radial and azimuthal polarizations and the electric field preserves cylindrical symmetry during propagation.

In [131], based on the method of the vector angular spectrum for electromagnetic beams and the method of the stationary phase, analytical vector formulas were obtained for describing the propagation of an annular beam in the far zone. Analytical expressions for finding the energy flow for TE- and TM-components and the entire annular beam in the far zone are presented. In [132], on the example of plane wave diffraction on a circular aperture in the near zone, a comparison of calculation algorithms using the vector integral Rayleigh-Sommerfeld transformation and expansion by plane waves was carried out in terms of accuracy and speed of calculations. A detailed analysis of the diffraction of a vortex beam at a circular aperture in the near zone was carried out using various calculation algorithms: vector integral Rayleigh-Sommerfeld transformation, expansion by plane waves, and the finite-difference time method [133]. Analytical expressions for the electromagnetic fields of radially polarized beams diffracted by a circular aperture are derived in [134] on the basis of Rayleigh's vector diffraction integral.

Analytical expressions for the electromagnetic fields of a cylindrically polarized vector beam propagating in free space were obtained in [135] on the basis of the vector angular spectrum and stationary phase methods. The analysis shows that azimuthal polarization in comparison with radial polarization is characterized by better energy focusing in the far zone. In [136], based on the angular spectrum method and the stationary phase

method, analytical expressions for studying the vector structure of a Gaussian beam diffracted at an aperture in the far zone were obtained in a rigorous form. In [137], based on the vector angular representation of the beam spectrum and the stationary phase method, an analytical expression for a cylindrically polarized Lager-Gaussian beam diffracted by a circular aperture in the far zone was obtained. The contribution of propagating waves and evanescent waves associated with nonparaxial light fields that propagate freely and in which the transverse component of the field is azimuthally polarized in an arbitrary plane was studied [138]. The analysis is carried out within the framework of the approach of the angular spectrum of plane waves. In [139], four fast and rigorous methods for modeling light propagation in a homogeneous medium are presented. It is shown that when studying the propagation of radiation beams in free space, analytical processing of rapidly oscillating phase components is very effective in reducing computational costs.

This section describes theoretical and experimental studies of the features of the structure of the field of laser radiation beams excited by the modes of the waveguide circular resonator of a THz laser in free space in diffraction zones with different types of spatial polarization of these modes.

3.2. PROPAGATION OF RADIATION OF TERAHERTZ LASER BASED ON A METALLIC CIRCULAR WAVEGUIDE IN DIFFERENT DIFFRACTION ZONES

3.2.1. Theoretical Relations

The propagation of laser radiation in free space along the Oz axis will be described by the well-known Rayleigh–Sommerfeld integrals [140]:

$$\begin{aligned}
 E_x(\vec{r}) &= -\frac{1}{2\pi} \iint_{\Sigma_0} E_x^0(\vec{r}_0) \frac{\partial}{\partial z} \left[\frac{\exp(ikR)}{R} \right] dx_0 dy_0, \\
 E_y(\vec{r}) &= -\frac{1}{2\pi} \iint_{\Sigma_0} E_y^0(\vec{r}_0) \frac{\partial}{\partial z} \left[\frac{\exp(ikR)}{R} \right] dx_0 dy_0, \\
 E_z(\vec{r}) &= \frac{1}{2\pi} \iint_{\Sigma_0} E_x^0(\vec{r}_0) \frac{\partial}{\partial x} \left[\frac{\exp(ikR)}{R} \right] dx_0 dy_0 + \frac{1}{2\pi} \iint_{\Sigma_0} E_y^0(\vec{r}_0) \frac{\partial}{\partial y} \left[\frac{\exp(ikR)}{R} \right] dx_0 dy_0,
 \end{aligned} \tag{3.1}$$

where $E_x^0(\vec{r}_0)$ and $E_y^0(\vec{r}_0)$ are the complex amplitudes of the x and y components of the input electric field is given, the z -component is assumed to be zero due to the choice of the coordinate system, \sum_0 is the area in which the input field is specified, $k = 2\pi / \lambda$ is the wave number, λ is the wavelength $\vec{r}_0 = x_0 \vec{e}_{x_0} + y_0 \vec{e}_{y_0}$, (x_0, y_0) are the Cartesian coordinates in the input plane, $\vec{r} = x \vec{e}_x + y \vec{e}_y + z \vec{e}_z$, (x, y, z) are the Cartesian coordinates in the observation plane, $R = \sqrt{(x - x_0)^2 + (y - y_0)^2 + z^2}$. Using the nonparaxial approximation (3.1), we expand R into a series, keeping its first and second terms in the form

$$R \cong r + \frac{x_0^2 + y_0^2 - 2xx_0 - 2yy_0}{2r}. \quad (3.2)$$

Substituting (3.2) into the rapidly oscillating integrals and into other places $R \cong r$, and passing to cylindrical coordinates, we obtain expressions for the field components in different diffraction zones:

$$\begin{aligned} E_x(\vec{r}) &= \frac{-z(ikr-1)}{2\pi r^3} e^{ikr} \times \\ &\quad \times \int_0^{2\pi} \int_0^\infty E_x^0(\vec{r}_0) \cdot \exp\left(\frac{ik\rho_0^2}{2r}\right) \cdot \exp\left(-ik \frac{\rho\rho_0 \cos(\varphi-\beta)}{r}\right) \rho_0 d\rho_0 d\varphi, \\ E_y(\vec{r}) &= \frac{-z(ikr-1)}{2\pi r^3} e^{ikr} \times \\ &\quad \times \int_0^{2\pi} \int_0^\infty E_y^0(\vec{r}_0) \cdot \exp\left(\frac{ik\rho_0^2}{2r}\right) \cdot \exp\left(-ik \frac{\rho\rho_0 \cos(\varphi-\beta)}{r}\right) \rho_0 d\rho_0 d\varphi, \quad (3.3) \\ E_z(\vec{r}) &= \frac{(ikr-1)}{2\pi r^3} \cdot e^{ikr} \times \\ &\quad \times \int_0^{2\pi} \int_0^\infty \left[E_x^0(\vec{r}_0)(\rho \cos\beta - \rho_0 \cos\varphi) + E_y^0(\vec{r}_0)(\rho \sin\beta - \rho_0 \sin\varphi) \right] \times \\ &\quad \times \exp\left(\frac{ik\rho_0^2}{2r}\right) \cdot \exp\left[-ik \frac{\rho\rho_0 \cos(\varphi-\beta)}{r}\right] \rho_0 d\rho_0 d\varphi. \end{aligned}$$

Here (ρ, β, z) are cylindrical coordinates in the observation plane and (ρ_0, φ) are polar coordinates in the region of the input field setting. In this

case $R \approx r + \frac{\rho_0^2 - 2\rho\rho_0 \cos(\varphi - \beta)}{2r}$.

The modes of the studied laser resonator coincide with the modes of a circular hollow dielectric waveguide. Let the given radiation in the initial plane be in the form of azimuthally symmetric TE_{0n} modes of a circular metal waveguide, the field components of which in the source plane $z = 0$ have the form:

$$\begin{aligned} E_x^0(\vec{r}_0, 0) &= -A_{0n} J_1\left(\frac{\chi'_{0n} \rho_0}{a}\right) \sin\varphi, \\ E_y^0(\vec{r}_0, 0) &= A_{0n} J_1\left(\frac{\chi'_{0n} \rho_0}{a}\right) \cos\varphi, \end{aligned} \quad (3.4)$$

where $A_{0n} = \frac{1}{(J_0(\chi'_{0n})\sqrt{\pi})a}$ is the normalizing factor, χ'_{0n} the n th root of

the equation $J'_0(\chi') = 0$. Using expression (3.3) and the reference integral $\int_0^{2\pi} \begin{Bmatrix} \cos(m\phi) \\ \sin(m\phi) \end{Bmatrix} \exp[-ix\cos(\phi - \theta)] d\phi = 2\pi(-i)^m J_m(x) \begin{Bmatrix} \cos(m\phi) \\ \sin(m\phi) \end{Bmatrix}$, we obtain

expressions for the field components in different diffraction zones:

$$\left\{ \begin{aligned} E_x(\vec{r}) &= -\frac{iz(ikr - 1)}{r^3} e^{ikr} \times \\ &\quad \times A_{0n} \sin\beta \int_0^a J_1\left(\frac{\chi'_{0n} \rho_0}{a}\right) e^{ik\frac{\rho_0^2}{2r}} J_1\left(\frac{k\rho_0\rho}{r}\right) \rho_0 d\rho_0, \\ E_y(\vec{r}) &= \frac{iz(ikr - 1)}{r^3} e^{ikr} \times \\ &\quad \times A_{0n} \cos\beta \int_0^a J_1\left(\frac{\chi'_{0n} \rho_0}{a}\right) e^{ik\frac{\rho_0^2}{2r}} J_1\left(\frac{k\rho_0\rho}{r}\right) \rho_0 d\rho_0, \\ E_z(\vec{r}) &= 0. \end{aligned} \right. \quad (3.5)$$

Next, we consider radiation in the initial plane in the form of radially symmetric TM_{0n} modes, whose field in the form of a source $z = 0$ has the form:

$$\begin{cases} E_x^0(\vec{r}_0, 0) = A_{0n} J_1\left(\frac{\chi_{0n} \rho_0}{a}\right) \cos\varphi, \\ E_y^0(\vec{r}_0, 0) = A_{0n} J_1\left(\frac{\chi_{0n} \rho_0}{a}\right) \sin\varphi, \end{cases} \quad (3.6)$$

where $A_{0n} = 1/(J_1(\chi'_{0n})\sqrt{\pi})a$ is the normalizing factor, χ_{0n} is the n th root of the equation $J_0(\chi_{0n}) = 0$. Then, using expression (3.3) and the above reference integral, we obtain expressions for the components of the field of these modes in the diffraction zones:

$$\begin{cases} E_x(\vec{r}) = \frac{iz(ikr-1)}{r^3} e^{ikr} A_{0n} \cos\beta \times \\ \quad \times \int_0^a J_1\left(\frac{\chi_{0n} \rho_0}{a}\right) e^{ik\frac{\rho_0^2}{2r}} J_1\left(\frac{k\rho_0\rho}{r}\right) \rho_0 d\rho_0, \\ E_y(\vec{r}) = \frac{iz(ikr-1)}{r^3} e^{ikr} A_{0n} \sin\beta \times \\ \quad \times \int_0^a J_1\left(\frac{\chi_{0n} \rho_0}{a}\right) e^{ik\frac{\rho_0^2}{2r}} J_1\left(\frac{k\rho_0\rho}{r}\right) \rho_0 d\rho_0, \\ E_z(\vec{r}) = \frac{(ikr-1)}{r^3} e^{ikr} A_{0n} \times \\ \quad \int_0^a J_1\left(\frac{\chi_{0n} \rho_0}{a}\right) e^{ik\frac{\rho_0^2}{2r}} \left[-i\rho J_1\left(\frac{k\rho_0\rho}{r}\right) - \rho_0 J_0\left(\frac{k\rho_0\rho}{r}\right)\right] \rho_0 d\rho_0. \end{cases} \quad (3.7)$$

We also consider radiation in the initial plane in the form of asymmetric TE_{1n} modes, the field of which in the source plane $z = 0$ has the form:

$$\begin{cases} E_x^0 = A_{1n} J_2\left(\frac{\chi_{1n} \rho_0}{a}\right) \sin 2\varphi, \\ E_y^0 = A_{1n} \left[J_0\left(\frac{\chi_{1n} \rho_0}{a}\right) - J_2\left(\frac{\chi_{1n} \rho_0}{a}\right) \right] \cos 2\varphi, \end{cases} \quad (3.8)$$

where $A_{1n} = \frac{1}{\left(J_2(\chi_{1n})\sqrt{2\pi(\chi_{1n}^2 - 1)}\right)a}$ is the normalizing factor, χ_{1n} is the n th root of the equation $J_1(\chi) = 0$.

Similarly, using expression (3.3) and the reference integral given above, we obtain the expression for the field components of these modes in the diffraction zones:

$$\left\{ \begin{array}{l} E_x(\vec{r}) = \frac{z(ikr-1)}{r^3} e^{ikr} A_{1n} \sin 2\beta \int_0^a J_2\left(\frac{\chi_{1n}\rho_0}{a}\right) J_2\left(\frac{k\rho_0\rho}{r}\right) e^{ik\frac{\rho_0^2}{2r}} \rho_0 d\rho_0, \\ E_y(\vec{r}) = -\frac{z(ikr-1)}{2\pi r^3} e^{ikr} 2\pi \int_0^a \left[J_0\left(\frac{\chi_{1n}\rho_0}{a}\right) J_0\left(\frac{k\rho_0\rho}{r}\right) - J_2\left(\frac{\chi_{1n}\rho_0}{a}\right) \times \right. \\ \quad \left. \times J_2\left(\frac{k\rho_0\rho}{r}\right) \cos 2\beta \right] e^{ik\frac{\rho_0^2}{2r}} \rho_0 d\rho_0, \\ E_z(\vec{r}) = \frac{ikr-1}{r^3} e^{ikr} A_{1n} \sin\beta \int_0^a \left[J_0\left(\frac{\chi_{1n}\rho_0}{a}\right) J_0\left(\frac{k\rho_0\rho}{r}\right) \rho - \right. \\ \quad \left. - i\rho J_0\left(\frac{\chi_{1n}\rho_0}{a}\right) + J_2\left(\frac{\chi_{1n}\rho_0}{a}\right) \right] \times \\ \quad \times \left[J_1\left(\frac{k\rho_0\rho}{r}\right) - \rho J_2\left(\frac{\chi_{1n}\rho_0}{a}\right) J_2\left(\frac{k\rho_0\rho}{r}\right) \right] e^{ik\frac{\rho_0^2}{2r}} \rho_0 d\rho_0. \end{array} \right. \quad (3.9)$$

To compare the spatial characteristics of the investigated modes and the modes of free space, we consider in the initial plane an axisymmetric Gaussian beam linearly polarized in the y direction, in which the field $E_0 = E_{0y}(\vec{r}_0, 0)\vec{y}$ in the source plane $z = 0$ has the form:

$$E_{0y}(\rho_0) = A_0 \exp\left(-\frac{\rho_0^2}{2w_{0I}^2}\right), \quad (3.10)$$

where $A_0 = \sqrt{\frac{2}{\pi}} \frac{1}{w_{0I}}$ is the normalizing factor, $w_{0I} = \frac{w'_{0I}}{a}$, w'_{0I} is the radius of the beam in terms of intensity at the e^{-1} level from its maximum value, and a is the radius of the waveguide.

Using expression (3.3), we obtain the final expression for the components of the radiation field of a Gaussian beam in free space in the form:

$$\left\{ \begin{array}{l} E_x(\vec{r}) = 0, \\ E_y(\vec{r}) = -\frac{z(ikr-1)}{2\pi r^3} e^{ikr} A_0 \int_0^a e^{-\frac{\rho_0^2}{2w_0^2}} e^{ik\frac{\rho_0^2}{2r}} J_0\left(\frac{k\rho_0\rho}{r}\right) \rho_0 d\rho_0, \\ E_z(\vec{r}) = -\frac{(ikr-1)}{r^3} e^{ikr} A_0 \sin\beta \times \\ \quad \times \int_0^a e^{-\frac{\rho_0^2}{2w_0^2}} \left[\rho J_0\left(\frac{k\rho_0\rho}{r}\right) + i\rho_0 J_1\left(\frac{k\rho_0\rho}{r}\right) \right] e^{ik\frac{\rho_0^2}{2r}} \rho_0 d\rho_0. \end{array} \right. \quad (3.11)$$

3.2.2. Comparison of Experimental and Numerical Results

Using the obtained expressions, the transverse distributions of the intensities of the waveguide modes during their propagation in free space were calculated. The calculation was performed for lower symmetric azimuthally (TE_{0n}) and radially (TM_{0n}) polarized modes and asymmetric (TE_{1n}) modes.

Experimental studies of the propagation of terahertz laser radiation in free space were carried out on the equipment, the structural diagram of which was given earlier in chapter 2 (Fig. 2.10). The laser resonator is formed by a hollow metal waveguide with a diameter of 19.92 mm and mirrors 17, 18. Mirror 17 is similar to the one described above, mirror 18 is mirror II (azimuthally symmetric diffraction grating with the parameters given in section 3. The radiation wavelength was chosen in the terahertz range $\lambda = 0.4326$ mm (generation line of a laser with optical pumping on the HCOOH molecule).

Figure 3.1 presents the experimental and calculated dependences of the half-width of the transverse distributions of intensity w at the level of $1/e^2$ on its maximum value for waveguide modes when the parameter ε , the inverse Fresnel number, changes ($\varepsilon = 1/N$, $N = a^2/\lambda L_1$, L_1 is the distance from the output end of the waveguide to the observation plane). The dependence for a Gaussian beam with a radius in the output plane of $w = 8.56$ mm, equal to the half-width of the TE_{01} waveguide mode at the open end of the waveguide at the $1/e^2$ level from the maximum intensity, is given here.

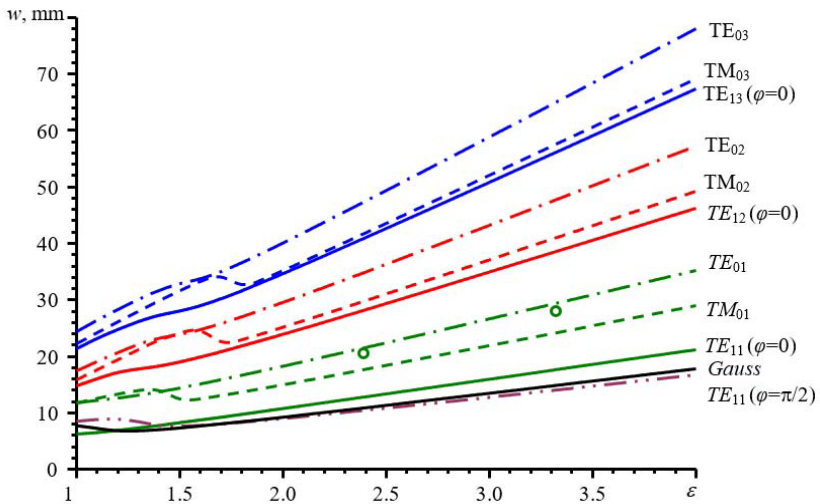


Figure 3.1. Calculated dependences of the half-width of the transverse intensity distributions w of the waveguide modes in free space when the parameter ε changes. Circles are an experiment

It can be seen from the given dependences that for small values of ε the changes in the width of the beams are nonlinear. In this region, the spatial transverse distribution of modes changes significantly (Figures 3.2 – 3.3).

The calculated and experimentally measured transverse intensity distributions of TE_{01} mode at a distance of 15 cm ($\varepsilon = 0.65$) and 100 cm ($\varepsilon = 4.36$) from the laser output mirror are shown in Figure 3.4. A good coincidence of the experimental and calculated curves is observed. Experimentally measured by the method of two intersections (points in Figure 3.1), the TE_{01} mode divergence of an optically pumped metal waveguide laser with the wavelength and waveguide radius given above is 0.035 rad. Good agreement was obtained between the measured and calculated beam divergences for the TE_{01} mode. For comparison, Figure 3.1 shows the dependence of the half-width of a Gaussian beam with a radius in the output plane equal to the half-width of the TE_{01} waveguide mode ($w = 8.56$ mm) at the open end of the waveguide, calculated according to formula (3.11).

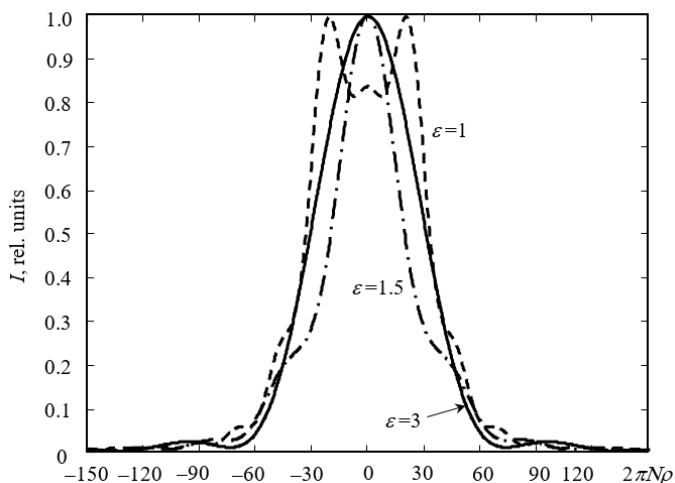


Figure 3.2. Relative transverse distributions of TE_{11} mode intensities at $\varphi = 0$

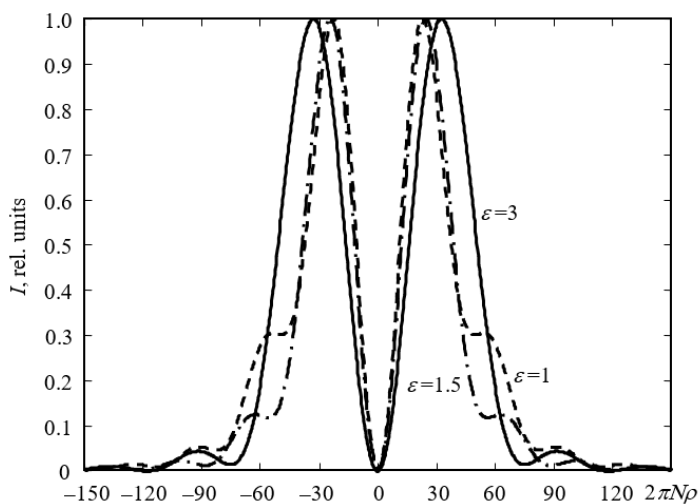


Figure 3.3. Relative transverse distributions of TM_{01} mode intensities

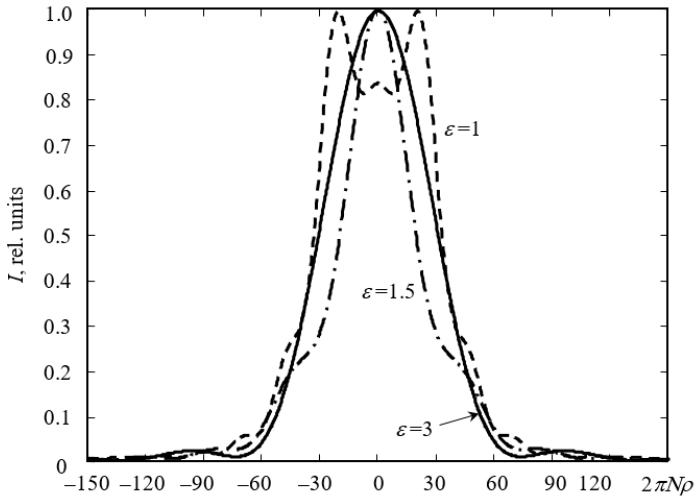


Figure 3.4. Relative transverse distributions of TE_{11} mode intensities at $\varphi = 0$

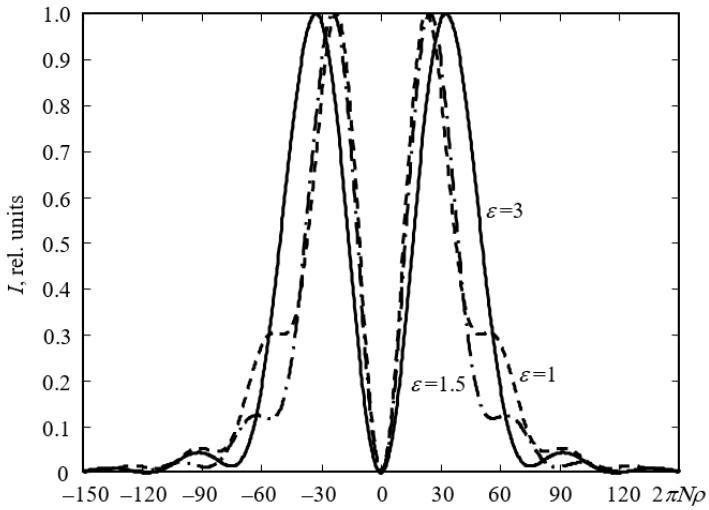


Figure 3.5. Relative transverse distributions of TM_{01} mode intensities

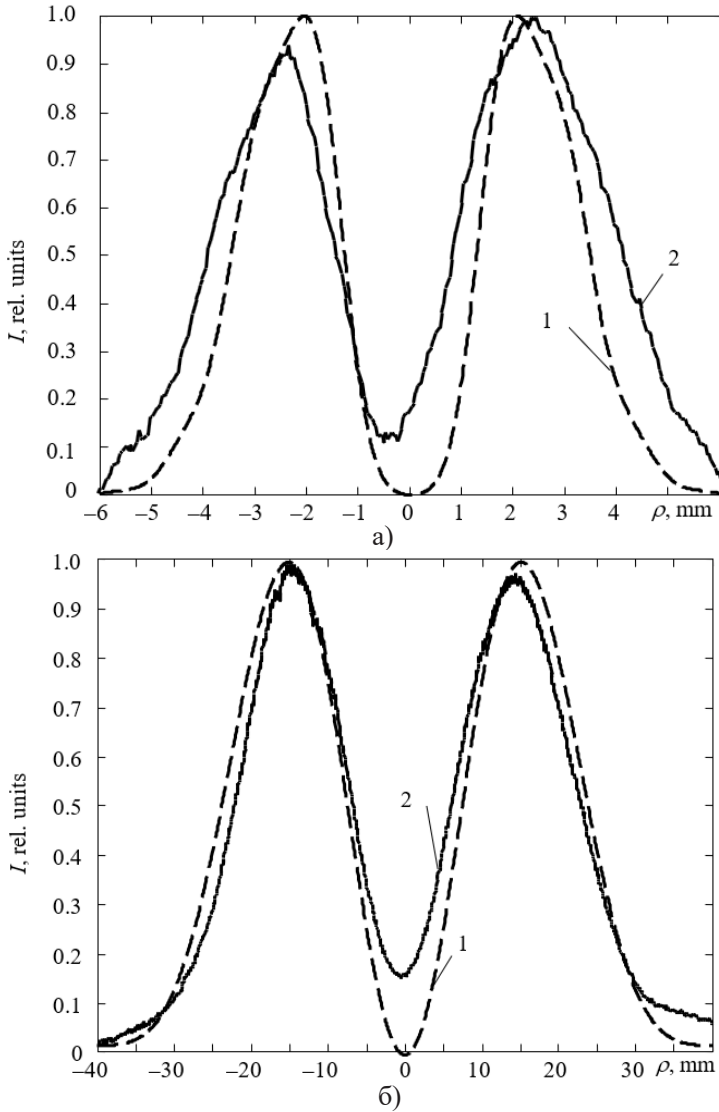


Figure 3.6. Calculated (1) and experimental (2) radial distributions of TE₀₁ mode field intensity at a distance of 15 cm (a) and 100 cm (b) from the laser output mirror

The angular divergence of the Gaussian beam calculated from the obtained data for $\varepsilon > 2$ was 0.0188 rad, and calculated by the well-known expression $\Theta = \lambda/\pi w = 0.0161$ rad [141]. The angular divergence Θ of the waveguide modes is given in Table 3.1.

Table 3.1

Angular divergence of waveguide modes

Type of mode	TE ₀₁	TE ₀₂	TE ₀₃	TM ₀₁	TM ₀₂	TM ₀₃	TE ₁₁	TE ₁₂	TE ₁₃	Gauss
Θ	0.037	0.061	0.084	0.031	0.053	0.075	0.029	0.049	0.065	0.019

The conducted theoretical and experimental comparison of the divergence of the TE₀₁ mode and the Gaussian beam allows us to conclude that the obtained analytical expressions in the nonparaxial approximation correctly describe the propagation of the modes of the metal waveguide resonator in free space. A stable field structure for symmetric and asymmetric modes in the terahertz range is observed at closer distances, in contrast to the distances predicted by the well-known criterion for the far diffraction zone.

3.3. PROPAGATION OF RADIATION OF TERAHERTZ LASER BASED ON A HOLLOW DIELECTRIC CIRCULAR WAVEGUIDE IN DIFFERENT DIFFRACTION ZONES

3.3.1. Theoretical Relations

We use the previously obtained expressions (3.3) in a cylindrical coordinate system [116; 142] to study the propagation in free space of the modes of a terahertz laser based on a circular dielectric waveguide. Let the given radiation in the initial plane be in the form of symmetric azimuthally, radially and linearly polarized TE_{0n}, TM_{0n}, EH_{1n} and asymmetric linearly polarized TE_{0n} + TH_{2n}, EH_{-1n} + EH_{3n} ($n = 1, 2$) modes of a circular hollow dielectric waveguide of radius a , the components of electromagnetic fields of which in the source plane $z = 0$ have a known form [50]. For TE_{0n} modes, the transverse components of the electromagnetic fields have the form:

$$\begin{cases} E_x^0(\vec{r}_0, 0) = -A_{0n} J_1\left(\frac{U_{0n} \rho_0}{a}\right) \sin\varphi, \\ E_y^0(\vec{r}_0, 0) = A_{0n} J_1\left(\frac{U_{0n} \rho_0}{a}\right) \cos\varphi, \end{cases} \quad (3.12)$$

where U_{0n} is the n th root of the equation $J_1(U_{0n}) = 0$, $A_{0n} = \frac{1}{\sqrt{\pi} |J_2(U_{0n})| a}$ is the normalizing factor.

For TM_{0n} modes, the transverse components of the electromagnetic fields have the following form:

$$\begin{cases} E_x^0(\vec{r}_0, 0) = A_{0n} J_1\left(\frac{U_{0n} \rho_0}{a}\right) \cos\varphi, \\ E_y^0(\vec{r}_0, 0) = A_{0n} J_1\left(\frac{U_{0n} \rho_0}{a}\right) \sin\varphi, \end{cases} \quad (3.13)$$

Transverse components of electromagnetic fields for EH_{1n} modes are presented in the following form:

$$\begin{cases} E_x^0(\vec{r}_0, 0) = A_{1n} J_0\left(\frac{U_{1n} \rho_0}{a}\right) \sin\varphi, \\ E_y^0(\vec{r}_0, 0) = A_{1n} J_0\left(\frac{U_{1n} \rho_0}{a}\right) \cos\varphi, \end{cases} \quad (3.14)$$

where U_{1n} is the n th root of the equation $J_0(U_{1n}) = 0$, $A_{1n} = \frac{1}{\sqrt{\pi} |J_1(U_{1n})| a}$ is the normalizing factor.

For $TE_{0n} + EH_{2n}$ mode, the transverse components of the electromagnetic fields have the form:

$$\begin{cases} E_x^0(\vec{r}_0, 0) = 0, \\ E_y^0(\vec{r}_0, 0) = A_{2n} J_0\left(\frac{U_{0n} \rho_0}{a}\right) \cos\varphi, \end{cases} \quad (3.15)$$

where $A_{2n} = \frac{\sqrt{2}}{\sqrt{\pi} |J_2(U_{0n})| a}$ is the normalizing factor.

For the $\text{EH}_{-1n} + \text{EH}_{3n}$ modes, the transverse components of the field are obtained as the sum of the corresponding components of the EH_{-1n} and EH_{3n} modes:

$$\begin{cases} E_x^0(\vec{r}_0, 0) = A_{3n} [1 + (-1)^n] J_{n+1}\left(\frac{U_{3n}\rho_0}{a}\right) \sin[(n+1)\varphi], \\ E_y^0(\vec{r}_0, 0) = A_{3n} [1 - (-1)^n] J_{n+1}\left(\frac{U_{3n}\rho_0}{a}\right) \cos[(n+1)\varphi], \end{cases} \quad (3.16)$$

where $A_{3n} = \frac{\sqrt{2}}{\sqrt{\pi}|J_2(U_{3n})|a}$ is the normalizing factor.

Using formula (3.3) for description the components of the electric field intensity vector that propagates, we obtain expressions for the transverse and longitudinal components of the field in an arbitrary plane $z = z_1$ in free space. For TE_{0n} mods, they look like this:

$$\begin{cases} E_x(\vec{r}) = \frac{-iz_1(ikr-1)}{r^3} e^{ikr} \times \\ \quad \times A_{0n} \sin\beta \int_0^a J_1\left(\frac{U_{0n}\rho_0}{a}\right) \exp\left(ik\frac{\rho_0^2}{2r}\right) J_1\left(\frac{k\rho_0\rho}{r}\right) \rho_0 d\rho_0, \\ E_x(\vec{r}) = \frac{iz_1(ikr-1)}{r^3} e^{ikr} \times \\ \quad \times A_{0n} \cos\beta \int_0^a J_1\left(\frac{U_{0n}\rho_0}{a}\right) \exp\left(ik\frac{\rho_0^2}{2r}\right) J_1\left(\frac{k\rho_0\rho}{r}\right) \rho_0 d\rho_0, \\ E_z(\vec{r}) = 0 \end{cases} \quad (3.17)$$

Similarly, the expressions for the field components of the TM_{0n} modes are obtained:

$$\left\{ \begin{aligned}
 E_x(\vec{r}) &= \frac{iz_1(ikr-1)}{r^3} e^{ikr} \times \\
 &\quad \times A_{0n} \cos\beta \int_0^a J_1\left(\frac{U_{0n}\rho_0}{a}\right) \exp\left(ik\frac{\rho_0^2}{2r}\right) J_1\left(\frac{k\rho_0\rho}{r}\right) \rho_0 d\rho_0, \\
 E_x(\vec{r}) &= \frac{iz_1(ikr-1)}{r^3} e^{ikr} \times \\
 &\quad \times A_{0n} \sin\beta \int_0^a J_1\left(\frac{U_{0n}\rho_0}{a}\right) \exp\left(ik\frac{\rho_0^2}{2r}\right) J_1\left(\frac{k\rho_0\rho}{r}\right) \rho_0 d\rho_0, \\
 E_z(\vec{r}) &= \frac{(ikr-1)}{r^3} e^{ikr} A_{0n} \sin\beta \int_0^a J_1\left(\frac{U_{0n}\rho_0}{a}\right) \exp\left(ik\frac{\rho_0^2}{2r}\right) \times \\
 &\quad \times \left[\rho_0 J_0\left(\frac{k\rho_0\rho}{r}\right) + i\rho J_1\left(\frac{k\rho_0\rho}{r}\right) \right] \rho_0 d\rho_0.
 \end{aligned} \right. \quad (3.18)$$

The expressions for the components field of the EH_{1n} modes have the following form:

$$\left\{ \begin{aligned}
 E_x(\vec{r}) &= 0, \\
 E_y(\vec{r}) &= \frac{-z_1(ikr-1)}{r^3} e^{ikr} A_{1n} \int_0^a J_0\left(\frac{U_{1n}\rho_0}{a}\right) \exp\left(ik\frac{\rho_0^2}{2r}\right) J_0\left(\frac{k\rho_0\rho}{r}\right) \rho_0 d\rho_0, \\
 E_z(\vec{r}) &= \frac{(ikr-1)}{r^3} e^{ikr} A_{1n} \sin\beta \int_0^a J_0\left(\frac{U_{1n}\rho_0}{a}\right) \exp\left(ik\frac{\rho_0^2}{2r}\right) \times \\
 &\quad \times \left[\rho J_0\left(\frac{k\rho_0\rho}{r}\right) + i\rho_0 J_1\left(\frac{k\rho_0\rho}{r}\right) \right] \rho_0 d\rho_0.
 \end{aligned} \right. \quad (3.19)$$

For $\text{TE}_{0n} + \text{EH}_{2n}$ modes the transverse and longitudinal components of the field are expressed in the following form:

$$\left\{ \begin{array}{l} E_x(\vec{r}) = 0, \\ E_y(\vec{r}) = \frac{iz_1(ikr-1)}{r^3} e^{ikr} \cos(\beta) A_{1n} \int_0^a J_0\left(\frac{U_{0n}\rho_0}{a}\right) \exp\left(ik\frac{\rho_0^2}{2r}\right) J_0\left(\frac{k\rho_0\rho}{r}\right) \rho_0 d\rho_0, \\ E_z(\vec{r}) = \frac{(ikr-1)}{r^3} e^{ikr} A_{1n} \sin(2\beta) \int_0^a J_1\left(\frac{U_{0n}\rho_0}{a}\right) \exp\left(ik\frac{\rho_0^2}{2r}\right) \times \\ \times \left[\rho_0 J_2\left(\frac{k\rho_0\rho}{r}\right) - i\rho J_1\left(\frac{k\rho_0\rho}{r}\right) \right] \rho_0 d\rho_0. \end{array} \right. \quad (3.20)$$

For the $\text{EH}_{-1n} + \text{EH}_{3n}$ modes the transverse and longitudinal components of the field have the form:

$$\left\{ \begin{array}{l} E_x(\vec{r}) = \frac{-z_1(ikr-1)}{r^3} e^{ikr} \left[1 + (-1)^n \right] \left[(-i)^{n+1} \right] \sin[(n+1)\beta] \times \\ \times \int_0^a J_{n+1}\left(\frac{U_{1n}\rho_0}{a}\right) J_{n+1}\left(\frac{k\rho_0\rho}{r}\right) e^{ik\frac{\rho_0^2}{2r}} \rho_0 d\rho_0, \\ E_y(\vec{r}) = \frac{-z_1(ikr-1)}{r^3} e^{ikr} \left[1 - (-1)^n \right] \left[(-i)^{n+1} \right] \cos[(n+1)\beta] \times \\ \times \int_0^a J_{n+1}\left(\frac{U_{1n}\rho_0}{a}\right) J_{n+1}\left(\frac{k\rho_0\rho}{r}\right) e^{ik\frac{\rho_0^2}{2r}} \rho_0 d\rho_0, \\ E_z(\vec{r}) = E_{z_1}(\vec{r}) + E_{z_{20}}(\vec{r}) + E_{z_{21}}(\vec{r}) + E_{z_3}(\vec{r}) + E_{z_{40}}(\vec{r}) + E_{z_{41}}(\vec{r}), \end{array} \right. \quad (3.21)$$

where

$$\begin{aligned} E_{z_1}(\vec{r}) &= \frac{(ikr-1)}{r^3} e^{ikr} \left[1 - (-1)^n \right] \left[(-i)^{n+1} \right] \sin[(n+1)\beta] \rho \cos(\beta) \times \\ &\times \int_0^a J_{n+1}\left(\frac{U_{1n}\rho_0}{a}\right) J_{n+1}\left(\frac{k\rho_0\rho}{r}\right) e^{ik\frac{\rho_0^2}{2r}} \rho_0 d\rho_0, \\ E_{z_{20}}(\vec{r}) &= \left[\frac{-(ikr-1)}{2r^3} e^{ikr} \right] \left[1 - (-1)^n \right] \left[(-i)^n \right] \sin(\beta) \times \\ &\times \int_0^a J_{n+1}\left(\frac{U_{1n}\rho_0}{a}\right) J_n\left(\frac{k\rho_0\rho}{r}\right) e^{ik\frac{\rho_0^2}{2r}} \rho_0^2 d\rho_0, \end{aligned}$$

$$\begin{aligned}
 E_{z_{21}}(\vec{r}) &= \left[\frac{-(ikr-1)}{2r^3} e^{ikr} \right] \left[1 - (-1)^n \right] \left[(-i)^{n+2} \right] \sin[(n+2)\beta] \times \\
 &\quad \times \int_0^a J_{n+1} \left(\frac{U_{1n}\rho_0}{a} \right) J_{n+2} \left(\frac{k\rho_0\rho}{r} \right) e^{ik\frac{\rho_0^2}{2r}} \rho_0^2 d\rho_0, \\
 E_{z_3}(\vec{r}) &= \left[\frac{(ikr-1)}{r^3} e^{ikr} \right] \left[1 - (-1)^n \right] \left[(-i)^{n+1} \right] \cos[(n+1)\beta] \rho \sin(\beta) \times \\
 &\quad \times \int_0^a J_{n+1} \left(\frac{U_{1n}\rho_0}{a} \right) J_{n+1} \left(\frac{k\rho_0\rho}{r} \right) e^{ik\frac{\rho_0^2}{2r}} \rho_0 d\rho_0, \\
 E_{z_{40}}(\vec{r}) &= \left[\frac{-(ikr-1)}{2r^3} e^{ikr} \right] \left[1 - (-1)^n \right] \left[(-i)^{n+2} \right] \sin[(n+2)\beta] \rho \cos(\beta) \times \\
 &\quad \times \int_0^a J_{n+1} \left(\frac{U_{1n}\rho_0}{a} \right) J_{n+2} \left(\frac{k\rho_0\rho}{r} \right) e^{ik\frac{\rho_0^2}{2r}} z_1 \rho_0^2 d\rho_0, \\
 E_{z_{41}}(\vec{r}) &= \left[\frac{(ikr-1)}{2r^3} e^{ikr} \right] \left[1 - (-1)^n \right] \left[(-i)^n \right] \sin(\beta) \times \\
 &\quad \times \int_0^a J_{n+1} \left(\frac{U_{1n}\rho_0}{a} \right) J_n \left(\frac{k\rho_0\rho}{r} \right) e^{ik\frac{\rho_0^2}{2r}} \rho_0^2 d\rho_0.
 \end{aligned}$$

To compare the spatial characteristics of the investigated modes and the modes of free space, we consider in the initial plane an axisymmetric Gaussian beam linearly polarized in the y direction, in which the field $E_0 = E_{0,y}(\vec{r}_0, 0) \vec{j}$ in the source plane $z = 0$ has the form:

$$E_{0,y}(\rho_0) = A_0 \exp\left(-\frac{\rho_0^2}{2w_{0I}^2}\right), \quad (3.22)$$

where $A_0 = \sqrt{2/\pi} \frac{1}{w_{0I}}$ is the normalization factor, $w_{0I} = \frac{w'_{0I}}{a}$, w'_{0I} is the radius of the beam in terms of intensity at the e^{-1} level from its maximum value, and a is the radius of the waveguide.

Using expression (3.3), we obtain the final expression for the components of the Gaussian beam radiation field in the form:

$$\left\{ \begin{array}{l} E_x(\vec{r}) = 0, \\ E_y(\vec{r}) = -\frac{z(ikr-1)}{2\pi r^3} e^{ikr} A_0 \int_0^a e^{-\frac{\rho_0^2}{2w_0^2}} e^{ik\frac{\rho_0^2}{2r}} J_0\left(\frac{k\rho_0\rho}{r}\right) \rho_0 d\rho_0, \\ E_z(\vec{r}) = -\frac{(ikr-1)}{r^3} e^{ikr} A_0 \sin\beta \times \\ \quad \times \int_0^a e^{-\frac{\rho_0^2}{2w_0^2}} \left[\rho J_0\left(\frac{k\rho_0\rho}{r}\right) + i\rho_0 J_1\left(\frac{k\rho_0\rho}{r}\right) \right] e^{ik\frac{\rho_0^2}{2r}} \rho_0 d\rho_0. \end{array} \right. \quad (3.23)$$

3.3.2. Comparison of Experimental and Numerical Results

Experimental studies of the propagation of THz laser radiation in free space were carried out on the setup, the structural diagram of which is given in section 2 (see Fig. 2.10). The laser resonator is formed by a hollow dielectric waveguide with a diameter of $2a = 35$ mm and mirrors 17, 18. The output mirror 18 was mirror II, made in the form of an azimuthally symmetric diffraction grating with the parameters given in section 2. Calculations and experiments were carried out at a wavelength of 0.4326 mm.

Using the obtained expressions, we calculated the transverse distributions of the field intensity of laser beams excited by symmetric azimuthally, radially and linearly polarized TE_{0n} , TM_{0n} , EH_{1n} and asymmetric linearly polarized $TE_{0n} + EH_{2n}$, $EH_{-1n} + EH_{3n}$ ($n = 1, 2$) modes of the dielectric waveguide resonator of a terahertz laser during their propagation in free space in near and far diffraction zones. Figures 3.7 – 3.12 show the transverse distributions of the field intensity of the given modes at different distances from the laser resonator.

Figure 3.13 presents the experimental and calculated dependences of the half-width of the transverse intensity distributions at the level of $1/e^2$ on its maximal value for waveguide modes when the parameter ε , the inverse Fresnel number, changes. It can be seen that when $\varepsilon < 2$, the transverse distribution of the mode intensity changes significantly. In the region $\varepsilon > 2$, the transverse profiles of the radiation beams acquire a stable structure, and only their width changes when ε increases.

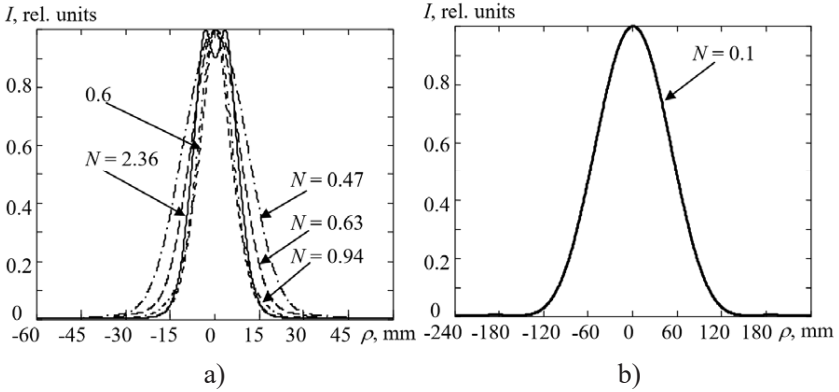


Figure 3.7. Transverse distributions of field intensity EH_{11} mode: a) in the near diffraction zone; b) in the far zone of diffraction

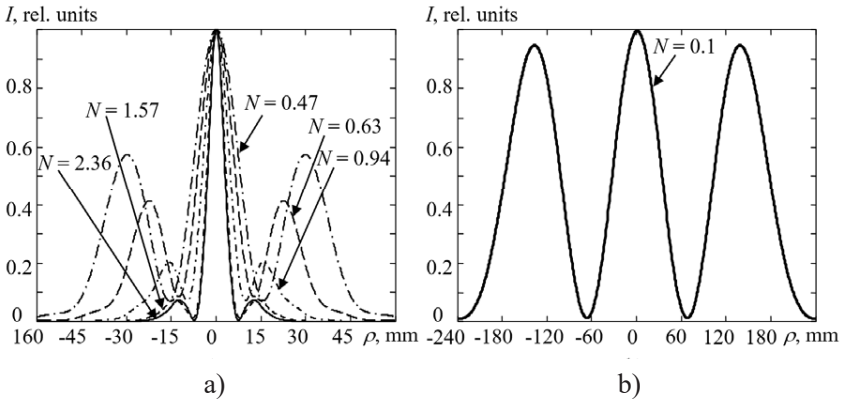


Figure 3.8. Transverse distributions of field intensity EH_{12} mode: a) in the near diffraction zone; b) in the far zone of diffraction

There is good agreement between experimentally measured (points in Figure 3.13) and calculated data for radiation beams excited by EH_{11} , $TE_{01}+EH_{21}$ modes. For comparison, the figure shows the dependence of the half-width of the Gaussian beam on the parameter ε . The radius of the beam is chosen equal to the radius of the EH_{11} mode at the $1/e^2$ level from its maximum value at the output end of the waveguide.

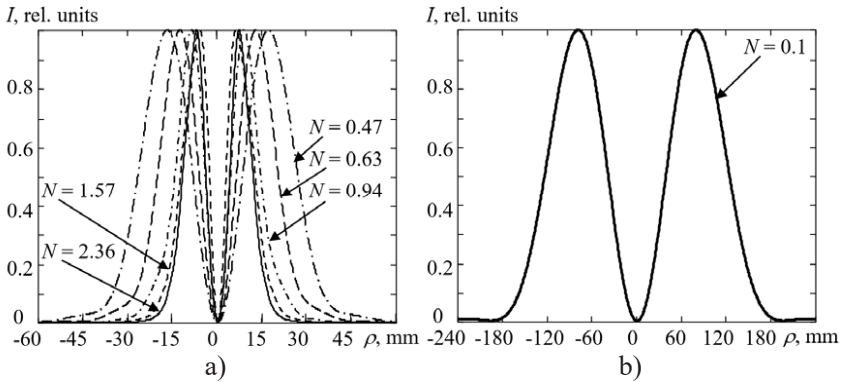


Figure 3.9. Transverse distributions of field intensity TE_{01} , TM_{01} , $TE_{01}+EH_{21}$ modes: a) in the near diffraction zone; b) in the far zone of diffraction

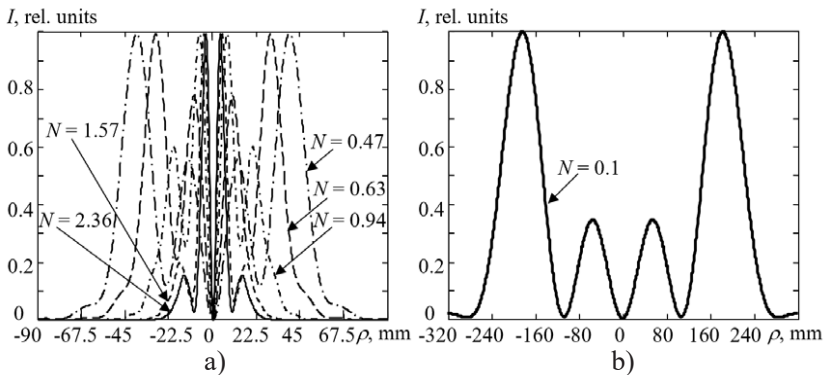


Figure 3.10. Transverse distributions of field intensity TE_{02} , TM_{02} , $TE_{02}+EH_{22}$ modes: a) in the near diffraction zone; b) in the far zone of diffraction

The experimentally obtained and calculated values of the divergence of laser beams in the far zone, obtained by the method of focal spot, for the modes EH_{11} and $TE_{01}+EH_{21}$ within the measurement error coincide and are shown in Table 3.2, where the calculated divergencies for other waveguide modes and the Gaussian beam are also given.

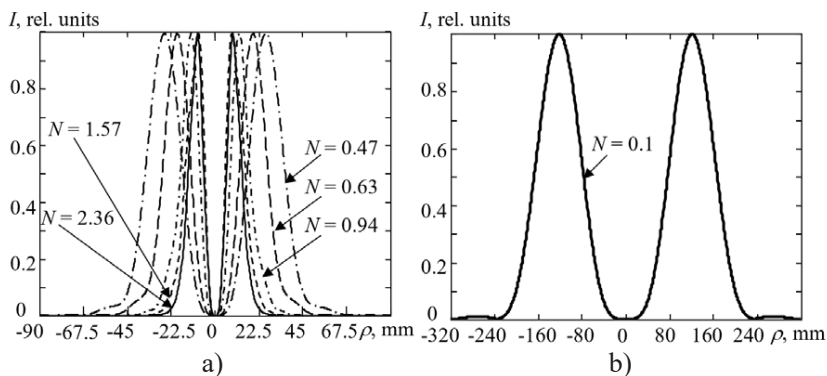


Figure 3.11. Transverse distributions of field intensity $EH_{-11} + EH_{31}$ modes:

a) in the near diffraction zone; b) in the far zone of diffraction

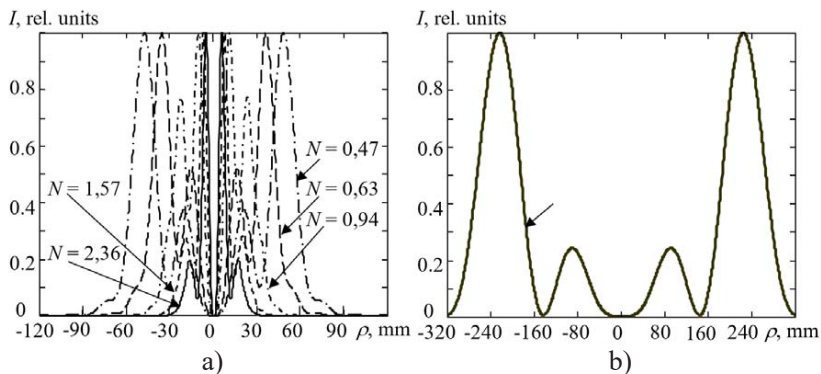


Figure 3.12. Transverse distributions of field intensity $EH_{-12} + EH_{32}$ modes:

a) in the near diffraction zone; b) in the far zone of diffraction

Table 3.2

Calculated divergencies of waveguide modes and Gaussian beam

Waveguide modes	TE ₀₁ TE ₀₂	TM ₀₁ TM ₀₂	EH ₁₁ EH ₁₂	TE ₀₁ + EH ₂₁ TE ₀₂ + EH ₂₂	EH ₋₁₁ + EH ₃₁ EH ₋₁₂ + EH ₃₂	Gaussian beam
Angular divergence Θ , rad.	0.0212 0.0334	0.0212 0.0334	0.0131 0.0293	0.0212 0.0334	0.0289 0.0371	0.011

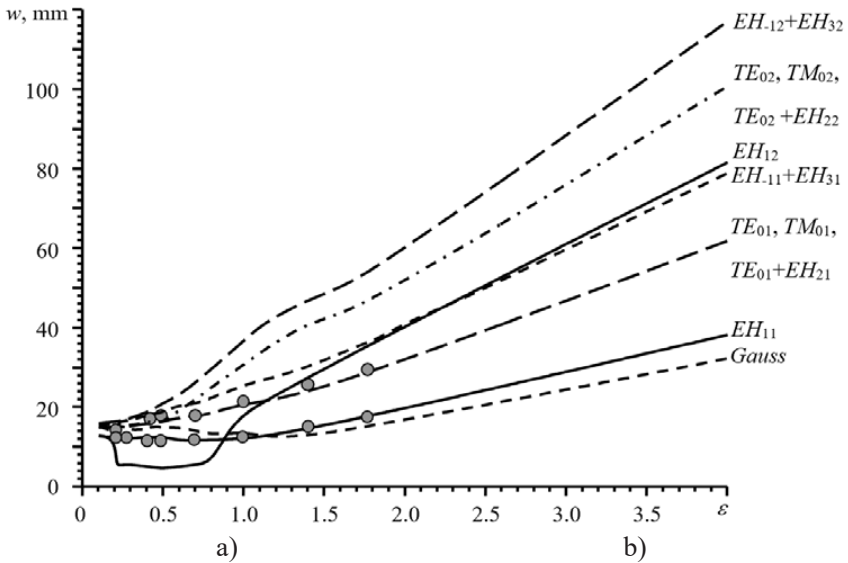


Figure 3.13. Calculated dependences of the half-width of the transverse intensity distributions w of the waveguide modes in free space when the parameter ε

These results allow us to conclude that the obtained analytical expressions in the nonparaxial approximation correctly describe the propagation of laser beams excited by the modes of the dielectric resonator of a terahertz laser with a circular waveguide in free space. At the same time, a stable field structure in free space for dielectric resonator modes in the terahertz range is observed at closer distances from the end of the waveguide ($L \geq 2a^2 / \lambda$) in contrast to the distances predicted by the well-known criterion ($L \geq 8a^2 / \lambda$) for the far diffraction zone [143].